

## A STUDY ON THE ENGINEERING PROPERTIES OF SAND IMPROVED BY THE SAND COMPACTION PILE METHOD

MUNENORI HATANAKA<sup>i)</sup>, LEI FENG<sup>ii)</sup>, NAOKI MATSUMURA<sup>iii)</sup> and HIROKI YASU<sup>iii)</sup>

### ABSTRACT

In order to directly evaluate the effects of soil improvement by the Sand Compaction Pile (SCP) method on the density, deformation, and static and liquefaction strength characteristics of sandy soils, a series of field and laboratory tests were performed. Laboratory tests were performed on high-quality undisturbed samples obtained from sandy soils both before and after soil improvement by the SCP method. The high-quality undisturbed samples were recovered by the in-situ freezing sampling method. The drained shear strength (internal friction angle,  $\phi_a$ ), liquefaction strength ( $R_{15}$ : cyclic stress ratio needed to cause 5% double amplitude axial strain in 15 cycles), and cyclic deformation characteristics ( $G \sim \gamma$  and  $h \sim \gamma$  relations) were determined by performing a series of laboratory tests on the undisturbed samples. Both the in-situ density and the relative density were measured on the undisturbed samples used in the laboratory tests. A standard penetration test (SPT) and a suspension-type P-S wave logging test were performed to investigate the soil profile of the test site before and after the sand compaction. Both the static and the liquefaction strengths of the sandy soils obtained in the laboratory tests were also compared with those estimated by empirical correlations used in practice based on the SPT  $N$ -value and soil gradations.

**Key words:** deformation characteristics, fines content, internal friction angle,  $K_o$ -value, liquefaction strength,  $N$ -value, relative density, sandy soils (IGC: D3/D6/D7)

### INTRODUCTION

The Sand Compaction Pile (SCP) method is an effective method by which to increase the density, rigidity, and static and the liquefaction strengths of sandy soils. The liquefaction strength, deformation characteristics, and in-situ density of sandy soils are significantly affected by the fabric structure of the soils. Due to the difficulty in obtaining high-quality undisturbed samples, few data on the directly measured engineering properties of sandy soils improved by the SCP method have been reported. Tokimatsu et al. (1990) and Okamura et al. (2004) reported the density and liquefaction strength of undisturbed sand samples only after sand compaction by the SCP method. The in-situ freezing sampling method is useful for obtaining high-quality undisturbed sand samples (Yoshimi et al., 1978; Hatanaka et al., 1995). The in-situ freezing method, however, is costly and time consuming. In most cases, it is difficult to use this method of sampling for soil survey in ordinary design applications. In practice, the effects of sand compaction on the engineering properties of sandy soils by the SCP method are usually indirectly estimated from the  $N$ -value obtained in standard penetration tests (SPT) conducted before and after sand compaction.

The present paper describes a case study to directly evaluate the effects of sand compaction by the SCP method on the density, deformation, and strength characteristics of sandy soils based on the test results of high-quality undisturbed samples recovered by the in-situ freezing sampling method before and after soil improvement by the SCP method. The applicability of some previous empirical correlations used in practice to estimate the strength of sandy soils based on the SPT  $N$ -value was also verified based on the obtained test results.

### SOIL PROFILE OF THE SAMPLING SITE AND SOIL IMPROVEMENT BY THE SAND COMPACTION PILE METHOD

Figure 1 shows the soil profiles of the sampling site and the SPT  $N$ -values obtained before and after the sand compaction. The sampling site is located at the east coast area of Tokyo bay. As shown in Fig. 1, the upper soil layer to a depth of approximately 6 m from the ground surface is a fill of fine sand, while the lower layer to a depth of approximately 11 m consists of an alluvial fine sand layer. The alluvial fine sand layer has some shell fragments at its lower boundary. There is also a thin silty clay layer between these two sand layers. The groundwater

<sup>i)</sup> Professor, Chiba Institute of Technology, Department of Architectural and Civil Engineering, Japan (Munenori.hatanaka@it-chiba.ac.jp).

<sup>ii)</sup> Graduate Student, ditto.

<sup>iii)</sup> Research Engineer, Tokyo Soil Research Co. Ltd., Japan (yasu@tokyosoil.co.jp).

The manuscript for this paper was received for review on April 26, 2006; approved on November 22, 2007.

Written discussions on this paper should be submitted before September 1, 2008 to the Japanese Geotechnical Society, 4-38-2, Sengoku, Bunkyo-ku, Tokyo 112-0011, Japan. Upon request the closing date may be extended one month.

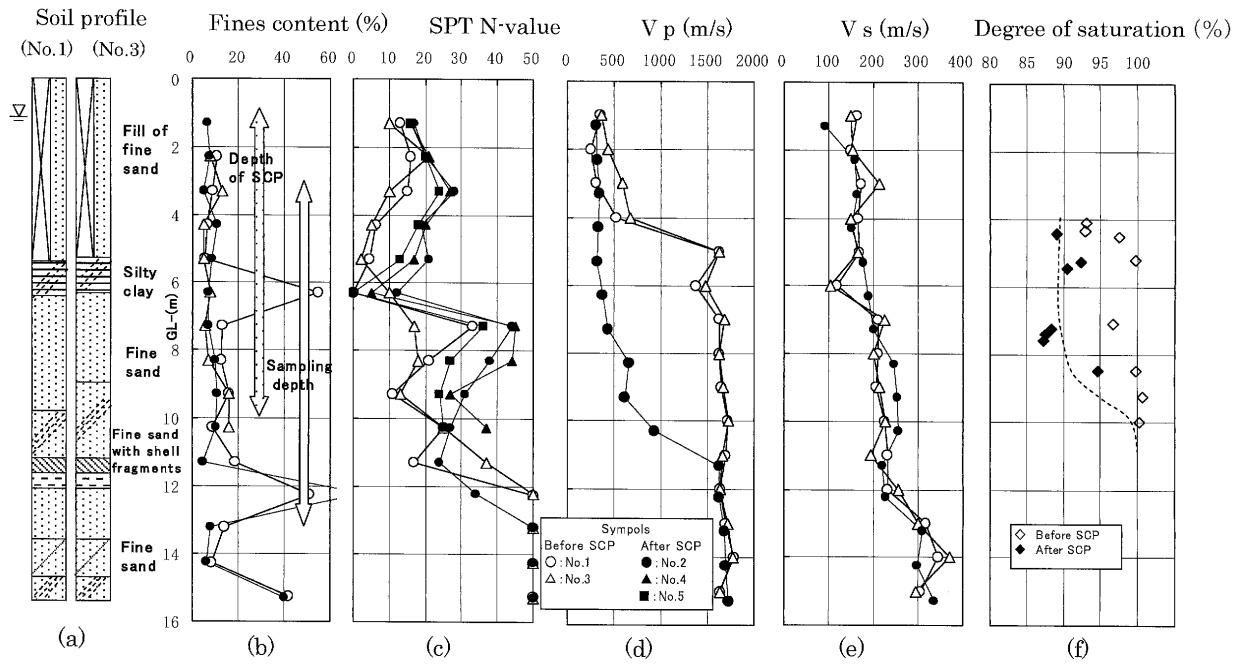


Fig. 1. Soil profile and field test results of sampling site

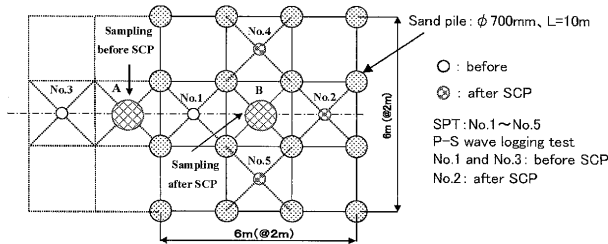


Fig. 2. Locations of sampling, field tests and sand piles performed by SCP method

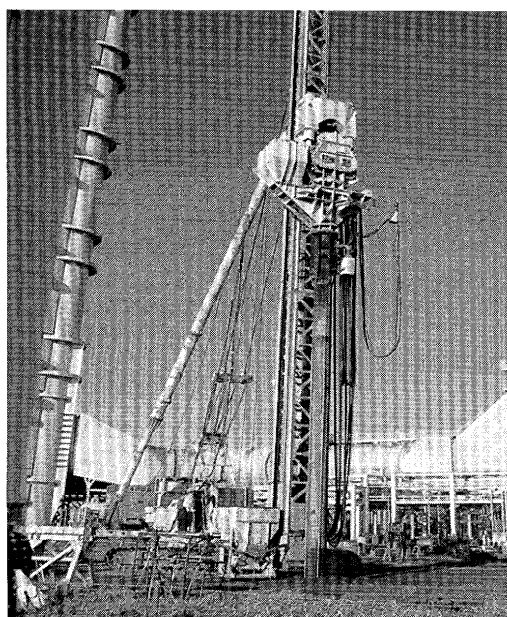


Fig. 3. Field performance of SCP

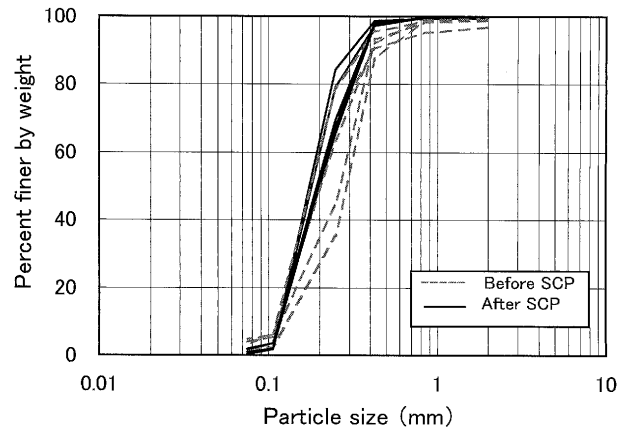


Fig. 4. Grain size distributions of undisturbed samples for upper sand fill

level is approximately 0.7 m from the ground surface. In order to evaluate the effects of sand compaction on sandy soils, sixteen sand piles were constructed at the site with a pile diameter of 700 mm and a pile interval of 2 m at depths of 1 to 10 m from the ground surface by the SCP method, as indicated in Figs. 1 and 2. The improvement ratio (the ratio between the cross sectional area of the sand piles and the area to be improved) is 9.6%. The sand of the sand piles was the same as the in-situ sand fill. Figure 3 shows the machine and the field performance of the SCP method used in the present study.

The soil gradations of the two sand layers were determined using undisturbed samples obtained both before and after the sand compaction, as shown in Figs. 4 and 5 respectively. As shown in Figs. 4 and 5, the fines and gravel contents (particle diameter: larger than 2.0 mm) of the undisturbed samples for the two sand layers are lower

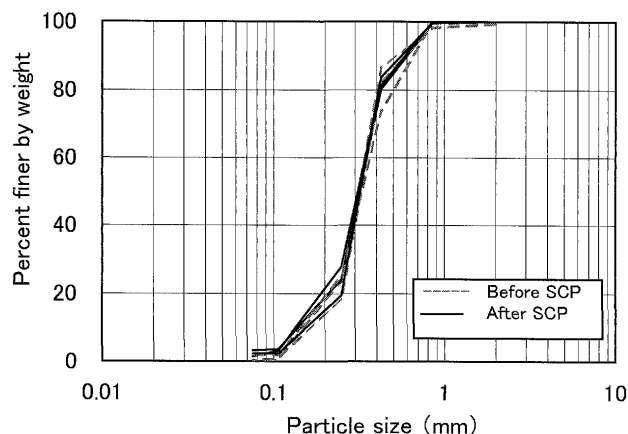


Fig. 5. Grain size distributions of undisturbed samples for lower alluvial sand

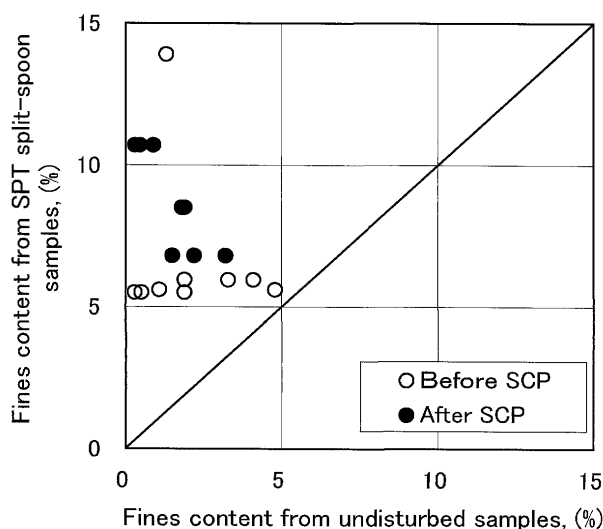


Fig. 6. Comparison of fines content between SPT split-spoon samples and undisturbed samples

than 5%. The sand layer of the sampling site consisted of clean sand. Most of the gravel contents consist of shell fragments. In addition, Fig. 4 indicates that the soil particles of the sand fill may be crushed by performing the SCP method by comparing the grain size distributions of samples before and after sand compaction. However, the effects of sand compaction on the particle crush of the lower alluvial sand layer were not significant. Figure 6 shows a comparison of the fines content between the undisturbed samples and the SPT split-spoon samples. As shown in Fig. 6, the fines contents of the undisturbed samples are far less than those of the SPT split-spoon samples. This is mainly due to the particle crush during the insertion of the split-spoon sampler into the ground (Hatanaka, M. and Feng, L., 2006).

## UNDISTURBED SAND SAMPLING AND FIELD INVESTIGATIONS

In order to obtain high-quality undisturbed sand sam-

ples, the in-situ freezing sampling method was performed. After a freezing pipe, 73 mm in outer diameter, was installed in a bored hole, the surrounding soil layer of approximately 800 mm in diameter was frozen using liquid nitrogen. Continuous undisturbed samples of sandy soils of 15 cm in diameter were recovered at depths of 3 to 13 m from the ground surface by using a double-tube core barrel (inner diameter: 150 mm) with diamond teeth from an undisturbed area approximately 10 cm from the freezing pipe at points A and B before and after the sand compaction, as indicated in Figs. 1 and 2, respectively. The details of the freezing and the sampling method are described in previous papers by the first author and his colleagues (Hatanaka et al., 1995; Hatanaka and Uchida, 1996).

In order to verify the applicability of some previous empirical correlations relating the SPT  $N$ -value and the strength of sandy soils used in design practice, standard penetration tests were performed at five locations before (Nos. 1 and 3) and after (Nos. 2, 4, and 5) the sand compaction, as shown in Figs. 1 and 2. From the viewpoint of conservatively estimating the effects of sand compaction on the SPT  $N$ -value, SPT was performed after the sand compaction at the midpoints between each of the four sand piles, as shown in Fig. 2. Figure 1 shows that the SPT  $N$ -value of sandy soils was increased by 5 to 20 by the sand compaction. However, there was no increase in the SPT  $N$ -value at the silty clay lying between two sand layers, as also shown in Fig. 1(c).

P-S wave logging tests using a suspension-type method were also performed by making use of the boring holes for SPT to measure the elastic wave velocity (Shear wave velocity,  $V_s$ , and Primary wave,  $V_p$ ) before (Nos. 1 and 3) and after (No. 2) the sand compaction, as shown in Figs. 1 and 2. Compared with the large increment of the SPT  $N$ -value due to the sand compaction, as shown in Fig. 1, the effects of the sand compaction on the shear wave velocity ( $V_s$ ) at depths of 1 to 5 m from the ground surface were not clear. The effects of the sand compaction on the shear wave velocity of the sand layer at a shallow depth remain unclear and should be studied continuously in detail.

On the other hand, the P-wave velocity ( $V_p$ ) was greatly decreased after the sand compaction at depths of 4 to 11 m from the ground surface. The depth corresponds approximately to the depth of the sand compaction, as shown in Fig. 1. This drastic decrease in the P-wave velocity after the soil improvement by the SCP method was caused by the decrease in the degree of saturation ( $S_v$ ) of the ground due to the air jetting used in performing the sand compaction, as reported by Okamura et al. (2004). The degree of saturation of the undisturbed samples recovered after the sand compaction was measured in the range of 87% to 95%, assuming that the degree of saturation of the sand before sand compaction below the ground water level was 100%, the volume expansion of the pore water due to the freezing was 9%, and they were fully drained during the freezing. Since only the effect of the sand compaction on the density and the fabric struc-

ture of soils were investigated in the present study, all of the undisturbed samples before and after the sand compaction were saturated in the laboratory again before testing. The effects of partial saturation of the sandy soils induced by the sand compaction pile method on the liquefaction strength are beyond the scope of the present study. They will be reported and discussed in another paper by the first author.

### EFFECTS OF SAND COMPACTION ON SOIL DENSITY

The dry density of the in-situ sandy soils was measured on the high quality undisturbed samples used in the laboratory tests. In order to obtain the relative density of sandy soils, the maximum and minimum dry densities of the samples were determined using the Japanese Industrial Standard Method of Test for the Maximum and Minimum Densities of Sand (JIS A1224, 2000). Figure 7 indicates the distributions of dry density before and after sand compaction with respect to depth. As shown in Fig. 7, the dry density of the upper sand fill before the sand compaction was very small, ranging only between 1.15 g/cm<sup>3</sup> and 1.35 g/cm<sup>3</sup>. In addition, as indicated in Fig. 7, for the upper loose sand fill, the dry density was significantly increased to approximately 1.41 to 1.51 g/cm<sup>3</sup> after the sand compaction. In the lower alluvial sand layer, the increment of the dry density was only 0.05 to 0.15 g/cm<sup>3</sup>. Figure 8 shows the distributions of the relative density with respect to depth before and after the sand compaction. The relative density of the upper sand fill before sand compaction was only 35% to 45%, which is very low. As a result, the sand fill layer without improvement may have a high potential of liquefaction during large earthquakes. In addition, as shown in Fig. 8, as a

result of the sand compaction, the relative density increased from approximately 45% to 65%, 36% to 75%, and 80% to 90%, at depths of 4.5 m, 5.5 m, and 7.5 m, respectively. In particular, the increase in the relative density in the loose sand fill was remarkable, which means that the Sand Compaction Pile Method is efficient for densifying loose sand layers.

### EFFECTS OF SAND COMPACTION ON CONSOLIDATED DRAINED STRENGTH

In order to study the effects of the sand compaction on the drained shear strength (internal friction angle,  $\phi_d$ ) of the sandy soils, the drained strength was determined by performing a series of consolidated drained triaxial compression tests (CD test) on the undisturbed samples obtained at three different depths before and after sand compaction. Three undisturbed samples, having diameters of 5 cm and lengths of approximately 12 cm, at each depth that were used for a series of CD tests were prepared from a frozen sand column of approximately 15 cm in both diameter and length. Using this method of sample preparation, it is expected that test samples can be obtained at a depth with fewer differences in soil gradations and densities for a series of tests.

The procedures of the CD test were as follows. The frozen sample was covered with a rubber membrane and sealed to the pedestal and top cup using O-rings after the sample was placed on the pedestal of a triaxial cell. The frozen specimen was then allowed to thaw in a drainable state under a confining stress of 19.6 kPa. After the sample was completely thawed, it was saturated with the aid of CO<sub>2</sub> gas, the deaired water and a back pressure of approximately 196 kPa, until the pore pressure coefficient  $B$ -value reached 0.95 or greater. Even though the undisturbed sand samples obtained after the soil improvement were not saturated due to the air jetting during the sand compaction as mentioned earlier, all of the samples used in the present study were fully saturated again before shearing. After saturation, each sample was isotropically consolidated at a specified effective confining stress. Since the coefficient of earth pressure at rest ( $K_0$  value) at sampling depth was not given in the present study, the minimum initial effective confining stress was set to the effective overburden stress at the sampling depth. The initial effective confining stress used in the CD test was 1, 2, 3, or 4 times the effective overburden stress at the sampling depth in order to remove the possible effect of the over consolidation on the drained strength. In this type of test method, this involves an inherent increase in sample density due to the different effective confining stress. In the present study, the increase in the relative density was a few points, and its effect on the drained strength was neglected. After consolidation, the sample was sheared in the drained condition. The depth of samples was tested and the test results obtained in the CD test are listed in Table 1. In Table 1, the relative densities are the average values of every three test samples at each depth. The SPT  $N$ -values at each depth are also the average values mea-

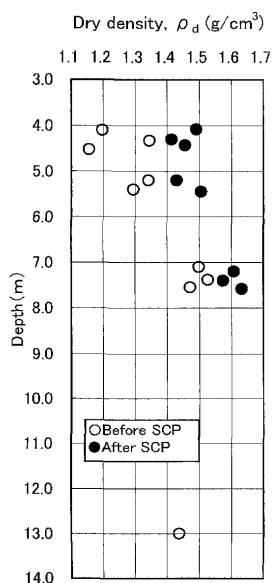


Fig. 7. Distributions of dry density with depth before and after SCP

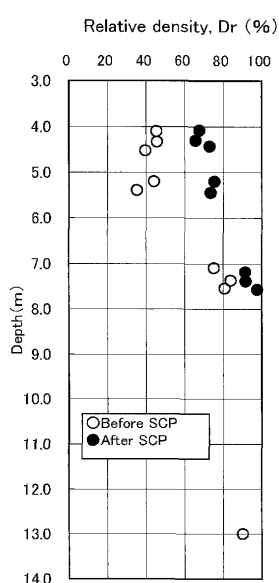
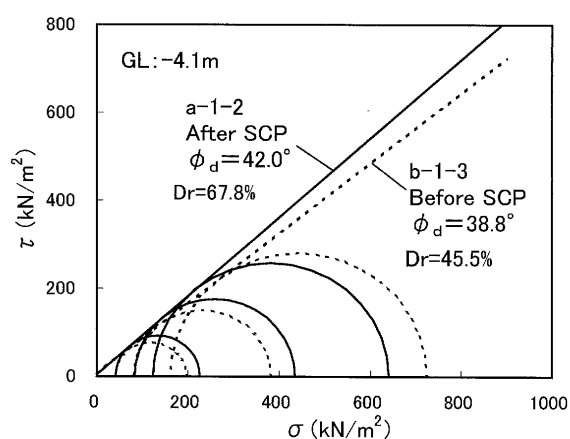
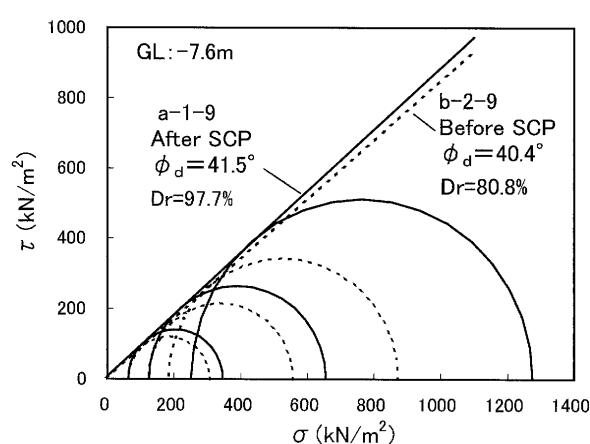
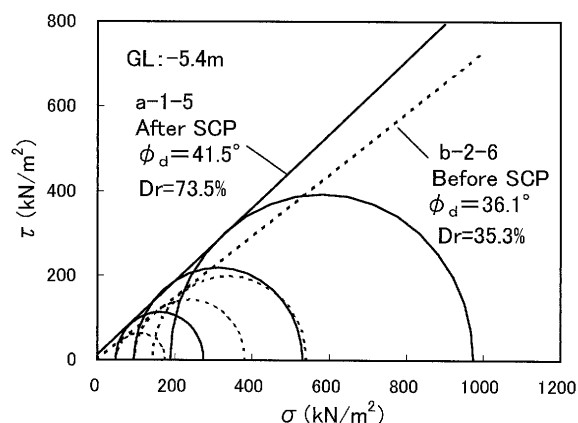


Fig. 8. Distributions of relative density with depth before and after SCP

**Table 1. Consolidated drained triaxial test results**

Soil condition	Sample No.	Depth (m)	Average relative density $D_r$ (%)	Average SPT $N$ -value	Effective overburden stress at sampling depth $\sigma'_v$ (kPa)	Internal friction angle $\phi_d$ ( $^\circ$ )
Before SCP	b-1-3	4.1	45.5	5.7	40.0	38.8
	b-2-6	5.4	35.3	4.6	47.0	36.1
	b-2-9	7.6	80.8	17.0	61.4	40.4
	b-2-16	13.0	90.3	91.0	106.2	44.8
After SCP	a-1-2	4.1	67.8	19.0	41.0	42.0
	a-1-5	5.5	73.5	17.0	47.0	41.5
	a-1-9	7.6	97.7	41.7	62.8	41.5

**Fig. 9. Mohr's circles at failure and internal friction angles (at -4.1 m)****Fig. 11. Mohr's circles at failure and internal friction angles (at -7.6 m)****Fig. 10. Mohr's circles at failure and internal friction angles (at -5.4 m)**

35% to 46%, increased significantly to 3.2 degrees and 5.4 degrees, respectively, due to the sand compaction. The effects of sand compaction on  $\phi_d$  of loose sandy soils are very large. The increase in the internal friction angle is very consistent with the increase in the relative density. These results indicate that the SCP method is useful for increasing the bearing capacity of loose sandy soils. In case of the alluvial sand layer at a depth of 7.6 m (Fig. 11), the increase in  $\phi_d$  ( $\phi_d$  before the sand compaction is  $40.4^\circ$ ) due to the sand compaction was approximately 1.1 degrees. The increase in  $\phi_d$  of the dense sand layer was far less than that of the upper loose sand fill. The difference in the increment of  $\phi_d$  between the two sand layers due to the sand compaction corresponds with the difference in the increment of the relative density between the two sand layers.

sured at boring holes Nos. 1 and 3, and Nos. 2, 4 and 5, before and after the sand compaction, respectively. At a depth of 13 m, because this depth is beyond the depth of the soil improvement by the SCP method, only the samples before the sand compaction were tested.

Figures 9 to 11 show Mohr's circles at failure and their envelopes of the undisturbed samples obtained before and after the sand compaction at depths of 4.1, 5.4, and 7.6 m from the ground surface, respectively. As shown in Figs. 9 and 10, the internal friction angle of the loose sand fill layer with a relative density of approximately

In design, the internal friction angle of sandy soils is often estimated based on the SPT  $N$ -value by using some empirical correlations. In Fig. 12, the test results before and after the sand compaction are shown with an empirical correlation relating  $N_1$  and  $\phi_d$ , as shown in Eq. (1). In Eq. (1),  $N_1$  is the normalized SPT  $N$ -value as defined by Eq. (2). This empirical correlation was originally proposed by Hatanaka and Uchida (1996) and Hatanaka et al. (1998) based on the test data for sandy soils with fines content lower than approximately 20% and  $\sigma'_v \geq 40$  kN/m<sup>2</sup>. In addition, this empirical correlation (Eq. (1)) was also adopted in the Recommendations for Design of

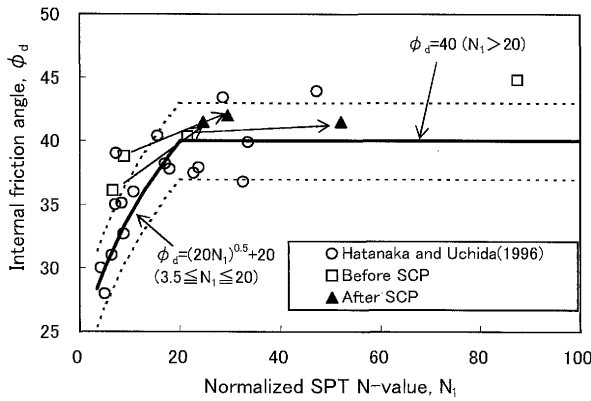


Fig. 12. Correlation between normalized SPT  $N$ -value,  $N_1$  and internal friction angle,  $\phi_d$

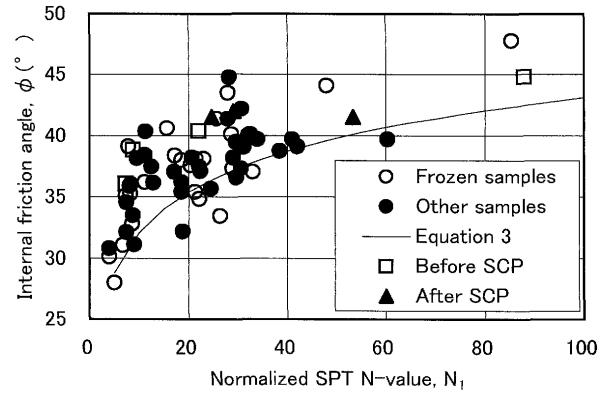


Fig. 13. Correlation between normalized SPT  $N$ -value,  $N_1$  (from Eq. (4)) and internal friction angle,  $\phi_d$  (Japan Highway Association, 2002)

Building Foundation (Architectural Institute of Japan, 2001). In the recommendations, in order to refrain from possible overestimation of the bearing capacity for a shallow foundation, normalization of the  $N$ -value with effective overburden stress ( $\sigma'_v$ ) is recommended for cases in which  $\sigma'_v$  exceeds 98 kN/m<sup>2</sup>.

$$\begin{aligned} \phi_d &= (20N_1)^{0.5} + 20 & 3.5 \leq N_1 \leq 20 \\ \phi_d &= 40 & 20 < N_1 \end{aligned} \quad (1)$$

$$N_1 = N(98/\sigma'_v)^{0.5} \quad \sigma'_v \geq 40 \text{ kN/m}^2 \quad (2)$$

As shown in Fig. 12, all the test data obtained in the present study show higher values of  $\phi_d$  than the estimation using Eq. (1), for a wide range of SPT  $N$ -value. This means that the drained shear strength of the sand fill both before and after the sand compaction and the alluvial sand can conservatively be estimated based on the normalized SPT  $N$ -value,  $N_1$ , by using Eq. (1). And as according to the recommendation of AIJ for the normalization of  $N$ -value only in the range of  $\sigma'_v \geq 98$  kN/m<sup>2</sup>, the test results of  $\phi_d$  will be much higher than the estimation by using Eq. (1) in the range of  $\sigma'_v$  between 40 kN/m<sup>2</sup> and 98 kN/m<sup>2</sup>. The test data were also plotted in Fig. 13, along with Eq. (3), which is recommended for designing the foundations of highway bridges in Japan.  $N_1$  in Eq. (3) is defined by Eq. (4). As shown in Fig. 13, Eq. (3) is also found to be very conservative for estimating the internal friction angle of sandy soils, even for larger values of  $N$ .

$$\phi_d = 4.8 \log N_1 + 21 \quad (3)$$

$$\begin{aligned} N_1 &= 170N/(\sigma'_v + 70) & \text{for } \sigma'_v \geq 50 \text{ kN/m}^2 \\ N_1 &= 170N/120 & \text{for } \sigma'_v < 50 \text{ kN/m}^2 \end{aligned} \quad (4)$$

Figure 14 indicates a pair of typical deviator stress-axial strain and axial strain-volumetric strain curves obtained in the CD tests for sand samples at depths of from 5.4 to 5.5 m before and after the sand compaction. Figure 14 clearly shows that, unlike the samples collected before the sand compaction, the deviator stress-axial strain curves of samples collected after the sand compaction had a higher and clearer peak stress. In addition, the

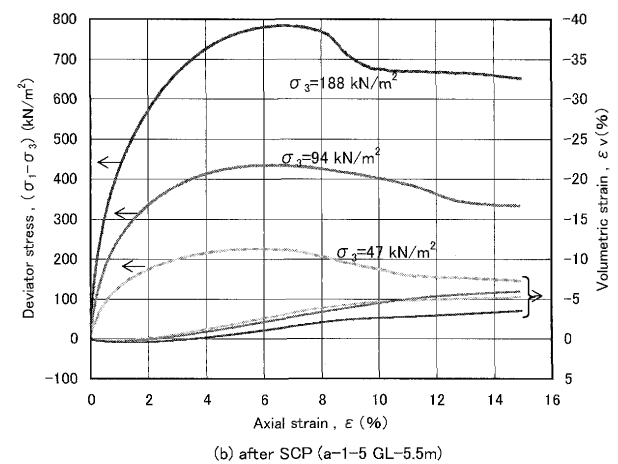
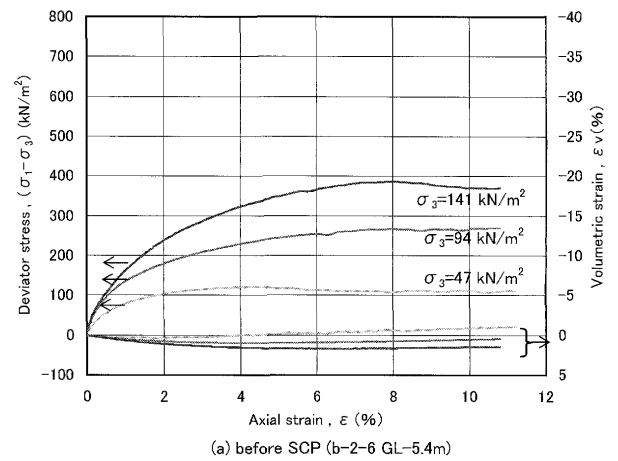


Fig. 14. Typical deviator stress-axial strain-volumetric strain relationships for samples before (a) and after (b) SCP obtained in CD test

volumetric strain of sand samples collected after sand compaction changed from compression to expansion at a much lower axial strain (approximately 1%) and reached a maximum volumetric expansion from 3% to 6%. This large volumetric expansion during drained shear for samples collected after the sand compaction corresponds with higher relative density and higher drained strength, as

Table 2. Liquefaction test results

Soil condition	Sample No.	Depth (m)	Relative density $D_r$ (%)	Average SPT $N$ -value	Effective overburden stress at sampling depth $\sigma'_v$ (kPa)	Average $F_c$ (%) from SPT sample	Adjusted $N$ -value, $N_a$ based on Eq. (6)	Adjusted $N$ -value, $N_{a(rs)}$ based on Eq. (10)	Liquefaction strength at 15 cycles
Before SCP	b-1-3-1	4.3	48.5	5.7	40.0	6.0	10.0	8.9	0.242
	b-1-3-2		45.5						0.172
	b-1-3-3		42.2						0.100
	b-1-3-4		46.5						0.126
After SCP	a-1-2-1	4.3	67.0	19.0	41.3	10.7	35.4	29.3	0.728
	a-1-2-2		65.0						0.606
	a-1-2-3		65.0						0.306
	a-1-2-4		65.9						0.182
Before SCP	b-2-5-1	5.2	43.8	4.6	47.0	5.6	7.3	6.6	0.146
	b-2-5-2		43.5						0.188
	b-2-5-3		43.5						0.134
	b-2-5-4		45.7						0.119
After SCP	a-1-5-1	5.2	70.7	17.0	47.0	8.5	28.7	24.5	0.196
	a-1-5-2		75.7						0.301
	a-1-5-3		76.8						0.513
	a-1-5-4		79.0						0.394
Before SCP	b-2-9-1	7.4	84.3	17.0	59.7	5.5	22.4	21.8	0.209
	b-2-9-2		88.3						0.334
	b-2-9-3		87.9						0.503
	b-2-9-4		75.4						0.628
After SCP	a-1-9-1	7.4	87.2	41.7	61.0	6.8	55.0	52.9	0.401
	a-1-9-2		92.2						0.695
	a-1-9-3		91.7						0.980
	a-1-9-4		95.6						1.491

shown in Figs. 8 and 9 to 11.

## EFFECTS OF SAND COMPACTION ON LIQUEFACTION STRENGTH

### Effects of Sand Compaction on Liquefaction Strength

The liquefaction strength of the in-situ sandy soils before and after sand compaction was determined in the laboratory by performing a series of consolidated undrained cyclic triaxial compression tests. Except for four undisturbed samples at each depth that were tested to obtain one liquefaction strength curve, the sample size and the methods of sample preparation, thawing, saturation, and consolidation used in the liquefaction test were the same as those for the CD test. In order to exclude the effect of partial saturation induced by air jetting during the SCP method, as described earlier, all of the undisturbed samples were saturated in the laboratory with a pore pressure coefficient  $B$ -value equal to or greater than 0.95. The liquefaction strength ( $R_{15}$ ) is defined as the cyclic stress ratio ( $\sigma_d/2\sigma'_{co}$ ,  $\sigma_d$ : deviator stress,  $\sigma'_{co}$ : initial effective confining stress,  $\sigma_{co} = \sigma'_v$  where  $\sigma'_v$  is the effective vertical stress at the sampling depth) needed to cause 5% double amplitude axial strain (DA) in 15 cycles. The test results are summarized in Table 2.

Figures 15 and 16 compare the time histories of the cyclic deviator stress, the axial strain, and the excess pore

Table 3. Cyclic deformation test results

Soil condition	Sample No.	Depth (m)	Average relative density $D_r$ (%)	Average $N$ -value	Effective overburden stress at sampling depth $\sigma'_v$ (kPa)
Before SCP	b-2-4	4.5	39.8	5.7	41.2
	b-2-8	7.1	75.3	17.0	58.8
After SCP	a-1-3	4.4	73.1	19.0	41.2
	a-1-9	7.2	91.6	36.0	58.8

water pressure ratio (a), the stress-strain curve (b), and the effective stress path (c) obtained in the liquefaction tests for samples obtained at a depth of 5.2 m before and after the sand compaction (data C and D as indicated in Fig. 18), respectively. Figures 15 and 16 show that even the cyclic stress and the initial effective confining stress (cyclic stress ratio) are approximately the same for the two samples, the rate of increase of the axial strain amplitude and the build up of the excess pore water pressure ratio was much slower for the sample collected after sand compaction. Compacted sand with a larger relative density is much harder and stronger with respect to undrained cyclic shearing.

Figures 17 through 19 compare the liquefaction strength curves between the samples collected before and after the sand compaction at depths of 4.3, 5.2, and

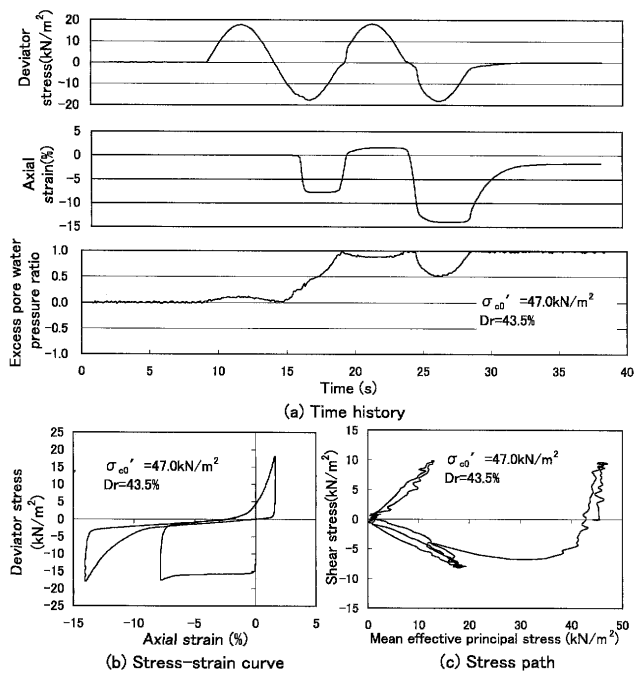


Fig. 15. Liquefaction test results of undisturbed sample C (Fig. 19) before SCP (at -5.2 m)

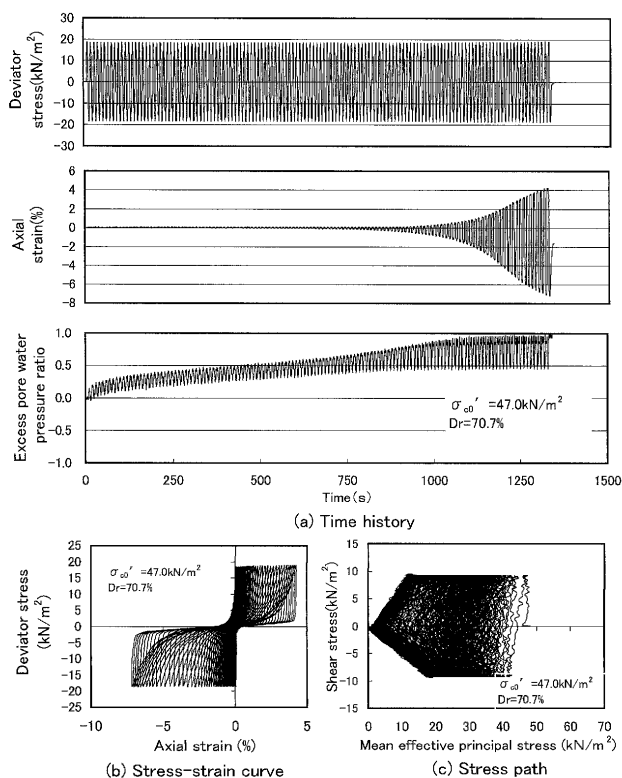


Fig. 16. Liquefaction test results of undisturbed sample D (Fig. 19) after SCP (at -5.2 m)

7.4 m from the ground surface, respectively. As shown in Figs. 17 to 19, the liquefaction strength at fifteen cycles of cyclic stress ( $R_{15}$ ,  $N_c = 15$ ) after the sand compaction was more than three times that before sand compaction. The effects of sand compaction by the SCP method on the

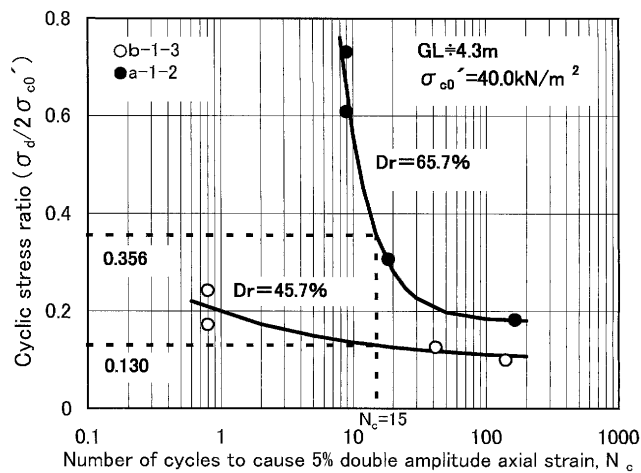


Fig. 17. Comparison of liquefaction strength for samples before and after SCP (at -4.3 m)

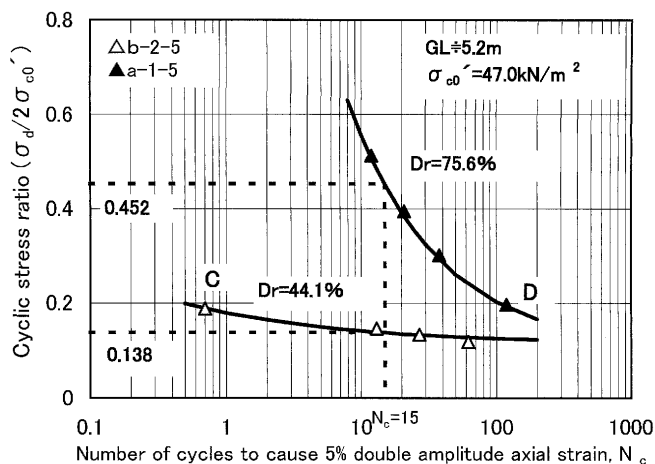


Fig. 18. Comparison of liquefaction strength for samples before and after SCP (at -5.2 m)

liquefaction strength were remarkable. In addition, the difference in the liquefaction strength between the samples before and after sand compaction is much larger for cases of fewer cycles ( $N_c \leq 10$ ), as shown in Figs. 17 through 19. This means that the effect of sand compaction on the liquefaction strength is much more significant for strong earthquakes with a shock type ground motion (an earthquake with few cycles of strong ground motion) (Ishihara, K. and Yasuda, S., 1975).

*Dr-Liquefaction Strength Correlation*

Figure 20 shows an empirical correlation between the relative density and the liquefaction strength ( $R_{15}$ ) for the high-quality undisturbed samples of clean sands with fines content lower than 5% obtained by the in-situ freezing method (Yoshimi, Y., 1994; Hatanaka et al., 1995). The test results of the liquefaction strength with the relative density obtained in the present study are also plotted in Fig. 20. The test results for the undisturbed samples before and after the sand compaction are very consistent with the previous  $D_r$ - $R_{15}$  correlation. The correlation

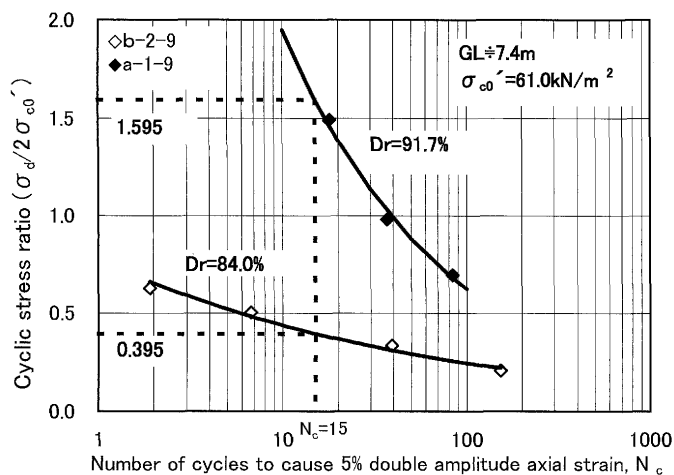


Fig. 19. Comparison of liquefaction strength for samples before and after SCP (at -7.4 m)

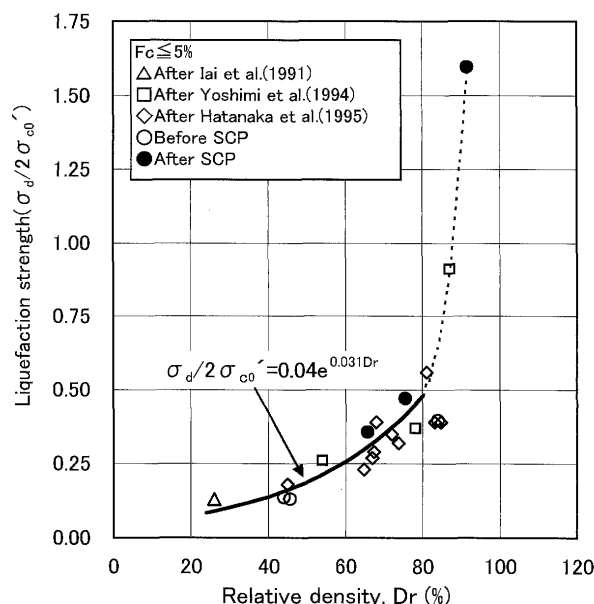


Fig. 20. Relationship between liquefaction strength and relative density for undisturbed samples obtained by in-situ freezing sampling method

shown in Fig. 20 between the relative density and  $R_{15}$  can be described as follows in the range of relative density lower than approximately 80%:

$$R_{15} = 0.04e^{0.031D_r} \quad (5)$$

where  $D_r$  is given as a percentage. This implies that the relative density can be a useful method for estimating the liquefaction strength of clean sands, if the in-situ relative density of clean sands can be reasonably estimated. It is also shown in Fig. 20 that the rate of the increase in liquefaction strength with the increase of the relative density in the range of  $D_r > 80\%$  is particularly large. This result suggests that for a seismic design with a larger design earthquake of level 2 (a very strong earthquake ground motion with a very low frequency of occurrence in the life cycle of a structure, but it is possible to occur

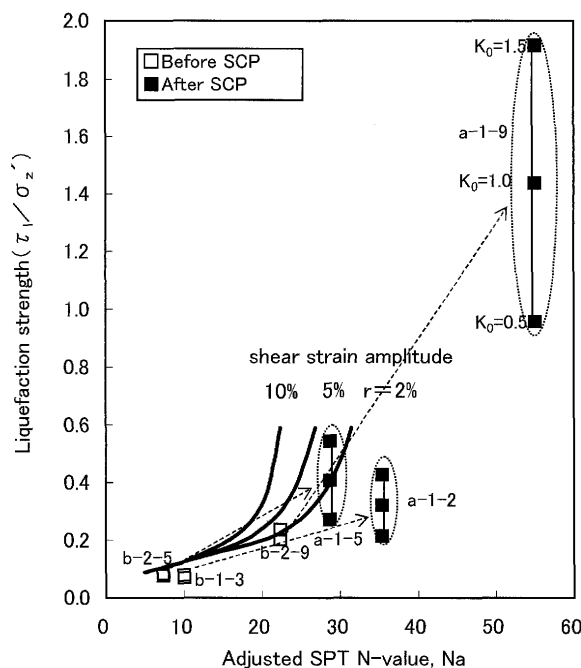


Fig. 21. Comparison of liquefaction strength between the test results and estimated value based on the adjusted SPT  $N$ -value,  $N_a$  (from Eq. (6)) (AIJ, 2001)

for a much longer time period), the SCP method may still be a very ductile method for mitigating disasters induced by sand liquefaction.

### Comparison of Liquefaction Strength between Test Results and Empirical Correlation

Figure 21 shows an empirical correlation (the curve for shear strain amplitude = 5%) between the in-situ liquefaction strength and the adjusted SPT  $N$ -value ( $N_a$ ) used in practice for estimating the in-situ liquefaction strength (Architectural Institute of Japan, 2001). The  $N_a$ - $R_{15}$  correlation for  $\gamma = 5\%$  shown in Fig. 21 is presented in the range of  $N_a$  smaller than 27 and is recommended in building foundation design. The maximum liquefaction strength for  $N_a = 27$  is approximately 0.6.  $N_a$  is defined in Eq. (6).  $N_1$  in Eq. (6) is the normalized SPT  $N$ -value as defined by Eq. (2), and  $\Delta N_f$  is defined by Eq. (7) based on the fines content of the SPT split-spoon samples.

$$N_a = N_1 + \Delta N_f \quad (6)$$

$$\Delta N_f = \frac{6}{5} F_c - 6 \quad 5\% \leq F_c < 10\%$$

$$\Delta N_f = \frac{1}{5} F_c + 4 \quad 10\% \leq F_c < 20\%$$

$$\Delta N_f = \frac{1}{10} F_c + 6 \quad 20\% \leq F_c \leq 50\% \quad (7)$$

where  $F_c$  is the fines content of SPT split-spoon samples given as a percentage.

$$\left(\frac{\tau_1}{\sigma_z}\right)_{(\text{In-situ})} = 0.9 \frac{1+2k_0}{3} \left(\frac{\sigma_d}{2\sigma'_o}\right)_{(\text{Laboratory test})} \quad (8)$$

$$K_o = 1 - \sin \phi_d \quad (9)$$

In order to compare the test results of undisturbed samples with the estimation based on the  $N_a$  value, the liquefaction strength ( $R_{15}$ ) obtained in the laboratory tests was converted to the in-situ liquefaction strength based on Eq. (8). The coefficient of earth pressure at rest  $K_o$  in Eq. (8) for samples before sand compaction was estimated at three depths based on Eq. (9) from the internal friction angle  $\phi_d$  obtained in CD test. The estimated  $K_o$ -values were 0.37, 0.41, and 0.35 at each respective depth. On the other hand, in practice, if there is no information about  $\phi_d$ , the  $K_o$  value for normally consolidated sand is often used as 0.5. In the present study, a  $K_o$  value between 0.5 and that calculated using Eq. (9) was adopted in converting the laboratory test results to in-situ strength. As shown in Fig. 21, the converted liquefaction strength of the undisturbed samples before sand compaction is slightly lower than that estimated from the  $N_a$  value defined by Eq. (6).

Next, the test results for undisturbed samples after sand compaction were compared. Several researchers have reported that the  $K_o$ -value increases due to sand compaction when performing the SCP method (for example, Ishihara, K. (1977), Ishihara et al. (1979) and Harada, K. et al. (2000)). Equation (9) is not adequate for estimating the  $K_o$ -value of compacted sand. Furthermore, there was no data of  $K_o$ -value at the test site after compaction. Based on the field test data of  $K_o$ -value reported by Harada, K. et al. (1997) on sandy soils improved by SCP method with the improvement ratio of 6 to 9%, in the present study, the liquefaction strength of the undisturbed samples after sand compaction was converted to the in-situ strength by assuming the  $K_o$  value after sand compaction to be in the range from 0.5 to 1.5. The converted in-situ liquefaction strength after sand compaction is also shown in Fig. 21. In the cases of samples No. a-1-2 (GL: -4.3 m) and No. a-1-5 (GL: -5.2 m), which were obtained at shallow depths, the  $N_a$  values after the sand compaction were 28.7 and 35.4 (larger than 27), and the converted in situ liquefaction strengths of these samples were much lower than 0.6, which is the estimation for  $N_a=27$  from the empirical correlation. This implies the possibility of overestimating the in-situ liquefaction strength in the case of such a large  $N_a$  value observed at a shallow depth using the empirical correlation. The overestimation of the  $N_a$  value may lead to the overestimation of the liquefaction strength. The reason for the difference between the converted results and the estimation of a larger  $N_a$  value, at shallow depths, will be discussed in the next section.

#### Discussion on the Effect of the Fines Content and Lateral Stress on the $N_a$ Value

As clearly shown in Figs. 17 through 19 and described earlier, the liquefaction strength ( $R_{15}$ ) of these samples increased approximately three to four times beyond that of the sand before compaction. The reason for the lack of agreement between the test results and the estimation is

thought to be mainly due to the inadequate assessment of  $N_a$  value observed at shallow depths for samples after sand compaction. The  $N_a$  value is a summation of the normalized SPT  $N$ -value,  $N_1$ , and the adjusted SPT  $N$ -value,  $\Delta N_f$ , as indicated in Eq. (7).

First, the method to adjust the  $N_1$  value based on the fines content of the SPT split-spoon samples is discussed. In a study on the method for estimating the relative density of sandy soils, Hatanaka and Feng (2006) reported that the method to adjust the SPT  $N$ -value based on the fines content of split-spoon samples using  $\Delta N_f$ , as proposed by Tokimatsu and Yoshimi (1983), as shown in Eq. (7), may be too large in the range of fines content between 5% and 15%. Hatanaka and Feng (2006) proposed Eq. (10) to adjust the relative density only for sands with fines content larger than 15%. In the present study, as shown in Table 2, the fines content ( $F_c$ ) of all of the SPT split-spoon samples at the depth of the samples tested was 6.0% to 10.7%, which is lower than 15%. By introducing Eq. (10) in the present study to adjust the  $N_1$  value, the modified  $N_a$  value for fines content,  $N_{a(Fc)}$ , was reduced from  $N_a$  value based on Eq. (7). The  $N_{a(Fc)}$  values at three depths before and after sand compaction are also listed in Table 2. As shown in Table 2, the fines content of samples after sand compaction is much larger than that of samples before compaction. As a result, the difference between  $N_a$  and  $N_{a(Fc)}$  is bigger for samples after compaction. The converted liquefaction strength was plotted with respect to the  $N_{a(Fc)}$  value, as shown in Fig. 22. The correlation between the converted liquefaction strength and the empirical correlation is improved especially for samples after sand compaction.

$$\Delta N_f = 0 \quad F_c \leq 15\% \quad (10)$$

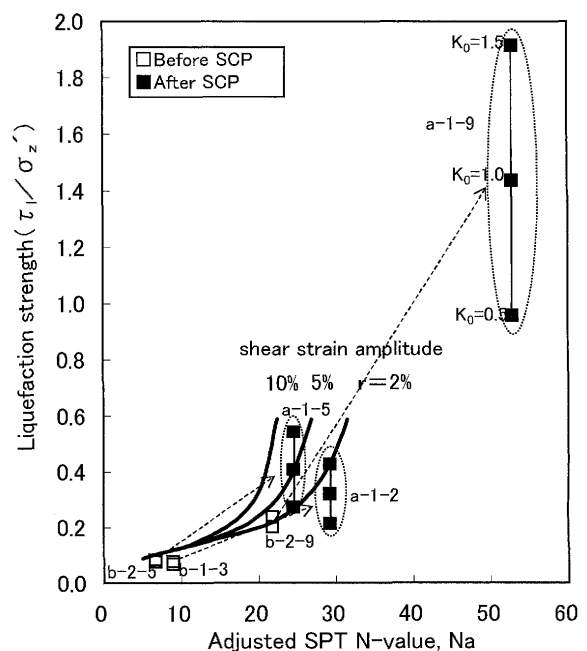


Fig. 22. Comparison of liquefaction strength between the test results and the estimated value based on the  $N_a$ -value modified for fines content ( $N_{a(Fc)}$ )

Next, the method to normalize the SPT  $N$ -value by using the overburden stress based on Eq. (2) is discussed. In converting the laboratory test result to in-situ liquefaction strength using Eq. (8), as described earlier, the effect of the sand compaction on the  $K_o$  value was taken into consideration (before sand compaction:  $K_o = 0.35\text{--}0.41$  to  $0.5$ ; after sand compaction:  $K_o = 0.5\text{--}1.5$ ). As indicated in Figs. 21 and 22, the effect of the  $K_o$ -value on the converted in-situ liquefaction strength is significant. For example, the in-situ liquefaction strength for  $K_o = 1.5$  is twice that for  $K_o = 0.5$ . The effect of increase in  $K_o$ -value due to sand compaction by SCP method was also reported by many researchers (for example, Harada et al., 1997; Ohbayashi et al., 1999). In determining the  $N_1$  value based on Eq. (2), however, the effect of sand compaction on  $K_o$  was not considered. In Eq. (2), the SPT  $N$ -value is normalized by the effective vertical stress ( $\sigma'_v$ ). It is reasonable to conclude, however, that the SPT  $N$ -value is essentially affected by the effective mean principal stress. It is better to normalize the SPT  $N$ -value by Eq. (11). The effective vertical stress is used in Eq. (2) because it is difficult to determine the lateral stress of in-situ sandy soils. Although the vertical stress is almost the same even after sand compaction at the same depth, the lateral stress must be increased due to sand compaction as reported by Ishihara et al. (1979). The lateral stress not only affects the converted liquefaction strength but also the normalized SPT  $N$ -value,  $N_1$ . If we do not consider the effect of the increase in the lateral stress on the  $N$ -value due to sand compaction, the normalized SPT  $N$ -value after sand compaction may be largely overestimated. In Eq. (2), the use of the effective vertical stress means that  $K_o$  is equal to 1.0. Here, for the purpose of verifying the effect of the lateral stress on the  $N_a$  value, the value of  $K_o$  after sand compaction is temporarily assumed to increase from 1.0 to 1.5 after sand compaction.

$$N_1 = N(98/\sigma'_{m0})^{0.5} \quad (11)$$

$$\sigma'_m = (1 + 2K_o)\sigma'_v/3 \quad (12)$$

where,  $\sigma'_m$  is mean effective stress.

The  $N_a$  value is reduced from 28.7 and 35.4 to 25.5 and 31.5 at these respective depths, and the modified  $N_a$  value for  $K_o$ -value,  $N_{a(K_o)}$ , is plotted in Fig. 23. Better consistency between the converted liquefaction strength and the empirical curve can be seen. However, there is still a difference. The application of the method for normalizing the SPT  $N$ -value by Eq. (2) for sandy soils after sand compaction, especially at shallow depths, should be studied in detail in the future.

As shown in Fig. 1, in the test field of the present study, the SPT  $N$ -value after sand compaction is much larger than 27 at depths shallower than 10 m from the ground surface. In such cases,  $N_a$  must be larger than 27, even without the adjustment for the fines content and the normalization by the confining stress. The limitations for the normalization of the SPT  $N$ -value by the overburden stress and the adjustment for the fines content should also be studied further.

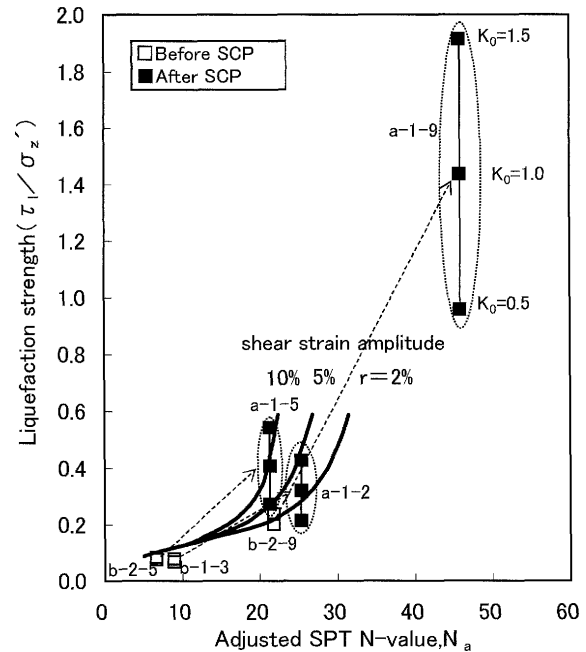


Fig. 23. Comparison of liquefaction strength between the test results and the  $N_a$ -value modified for  $K_o$  value ( $N_{a(K_o)}$ )

#### EFFECTS OF SAND COMPACTION ON THE CYCLIC DEFORMATION CHARACTERISTICS

In order to study the effects of sand compaction on the shear modulus ( $G$ ), the damping ratio ( $h$ ), and the strain ( $\gamma$ ) dependence of  $G$  and  $h$  of sandy soils, the  $G \sim \gamma$  and  $h \sim \gamma$  relations of sand samples before and after the sand compaction were obtained in a series of undrained cyclic triaxial deformation tests. The method of sample preparation, saturation and consolidation was essentially the same as that used in the liquefaction test. In these tests, a sample was cyclically sheared under the undrained condition at approximately ten different levels of shear strain in the order of smaller strain levels. At each strain level, ten cycles of constant amplitude cyclic stress was applied to the sample under the undrained condition. After ten cycles of undrained cyclic shear at each level, the sample was consolidated again under the drained condition. The test then proceeded to the next step with a larger level of shear strain under the undrained condition.

$$G = E/(2(1 + \nu)) \quad (13)$$

Shear modulus  $G$  is converted from Young's modulus ( $E$ ), assuming the Poisson's ratio ( $\nu$ ) to be 0.5 for the undrained condition from Eq. (13). Figures 24 and 25 show the comparisons of  $G \sim \gamma$  and  $h \sim \gamma$  relations of the undisturbed samples before and after sand compaction from the sand fill layer and the alluvial sand layer, respectively. As shown in Figs. 24 and 25, the shear modulus increased approximately 40% after sand compaction with increasing relative density. The effects of sand compaction on the shear modulus were also very large. The effects of sand compaction on the damping ratio, however, were much smaller than those on the shear modulus. In design practice, the effects of sand compac-

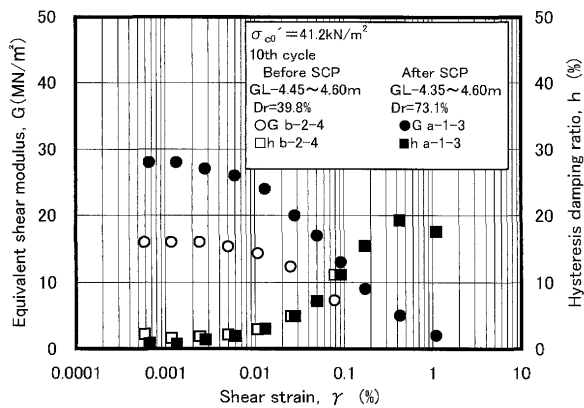


Fig. 24. Comparisons of  $G \sim \gamma$  and  $h \sim \gamma$  relations of undisturbed samples before and after SCP at sand fill layer

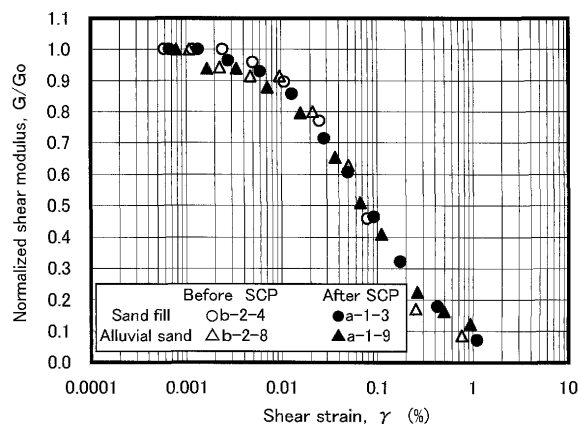


Fig. 26.  $G/G_0 \sim \gamma$  correlations for undisturbed samples before and after SCP

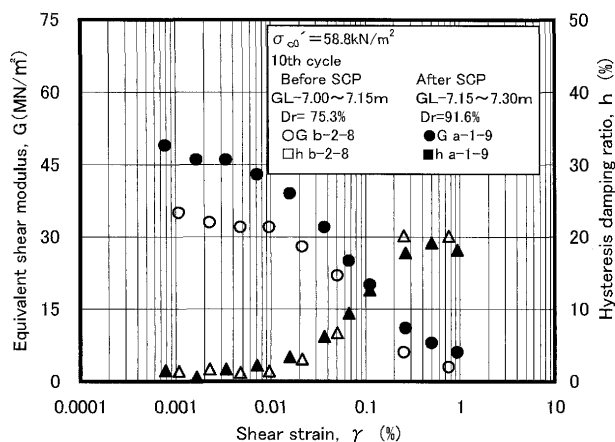


Fig. 25. Comparisons of  $G \sim \gamma$  and  $h \sim \gamma$  relations of undisturbed samples before and after SCP at alluvial sand layer

tion on the damping ratio may be neglected. Figure 26 indicates the correlations between the normalized shear modulus  $G/G_0$  (shear modulus at small strain level) and the shear strain  $\gamma$  for the undisturbed samples obtained before and after sand compaction from both sand layers. Even though the shear modulus was strongly affected by sand compaction, the effects of sand compaction on the  $G/G_0 \sim \gamma$  correlation were almost negligible. Moreover, there is no difference in the  $G/G_0 \sim \gamma$  correlations between the loose sand fill and the alluvial sand layer.

The shear modulus at the small strain level ( $G_0$ ) can also be obtained based on the elastic wave propagation theory from the shear wave velocity ( $V_s$ ) measured in the field and the unit weight of soils (Eq. (13)). In the present study, the values of  $G_0$  obtained in the laboratory tests for the samples at depths of 4.5 m and 7.2 m were approximately 45% and 70%, respectively, of the values calculated from the shear wave velocity before and after the sand compaction. Compared to the difference in  $G_0$  obtained in the laboratory for samples before and after sand compaction, as shown in Figs. 24 and 25, the difference in  $G_0$  calculated from the shear wave velocity measured in the field before and after sand compaction was much smaller because the shear wave velocity after sand

compaction increased only slightly, as described earlier herein. Unlike the other engineering properties, as shown in previous sections, the reason why only the shear wave velocity was unaffected by the sand compaction at shallow depths remains unclear and should be investigated in future studies.

$$G_0 = (\gamma_l/g)V_s^2 \quad (14)$$

where  $\gamma_l$  is the unit weight of soil mass,  $g$  is the acceleration of gravity, and  $V_s$  is the shear wave velocity.

## CONCLUSIONS

In order to directly evaluate the effects of sand compaction on the sandy soils by the Sand Compaction Pile method, the densities, deformation characteristics, and static and liquefaction strengths of the sandy soils before and after sand compaction at a clean sand site with a fines content lower than 5% were compared by performing a series of laboratory tests on the high-quality undisturbed samples recovered by the in-situ freezing sampling method. A series of standard penetration tests and P-S wave logging tests were also performed in order to investigate the soil profile of the test site and confirm the applicability of the previous empirical correlations used in practice to estimate the strength of sandy soils. The following results were obtained:

- 1) The SCP method increased the SPT  $N$ -value in the range of 5 to 20. Both the dry density and the relative density of sandy soils significantly increased by sand compaction. Not only a loose sand fill, but also an alluvial sand layer in a middle dense state ( $D_r=75\%$ ), were densified in 10 to 20 points of the relative density. The maximum increment of the relative density was 39 points. The increase of the SPT  $N$ -value corresponds well with the increase of the in-situ soil density.
- 2) Improvement by the Sand Compaction Pile method increased the drained shear strength (internal friction angle,  $\phi_d$ ) of sandy soils with increasing soil density. Especially for loose sandy soils, the increment of the internal friction angle was  $3^\circ$  to  $5^\circ$ . The test results for

the  $N_1$  (as defined by Eq. (2))– $\phi_d$  relation are found to be conservative compared with Eq. (1) in a wide range of  $N$ -value. The test results are much more conservative compared with the empirical correlation according to the recommendation of Architectural Institute of Japan (2001) in the range of  $\sigma'_v$  from 40 kN/m<sup>2</sup> to 98 kN/m<sup>2</sup>. The empirical correlation between  $N_1$  and  $\phi_d$  used in the foundation design of highway bridges in Japan is also found to be very conservative in a wide range of  $N_1$  values defined by Eq. (4).

- 3) The liquefaction strength ( $R_{15}$ : the cyclic stress ratio needed to cause 5% double amplitude axial strain in 15 cycles) of both the sand fill and the alluvial sand after sand compaction drastically increased to more than three times those before sand compaction with increasing relative density. The test results were also consistent with the empirical correlation between the relative density and the liquefaction strength for clean sand reported by Yoshimi (1994) and Hatanaka et al. (1995). The correlation between the relative density and the liquefaction strength ( $R_{15}$ ) can be expressed by Eq. (7). The rapid increase in the liquefaction strength of sandy soils in the range of relative density larger than 80% by sand compaction is very important for sandy soils to resist the enormous design earthquake ground motion of a level 2 earthquake (a very strong earthquake ground motion with a very low frequency of occurrence in the life cycle of a structure, but it is possible to occur in a much longer time period).

The liquefaction strength of the sandy soils before sand compaction was slightly lower than the estimation based on the previous empirical correlation (AIJ, 2001). The liquefaction strengths of sandy soils after sand compaction, especially at shallow depths, was not in agreement with the empirical correlation mainly due to the extremely large adjusted SPT  $N$ -value,  $N_a$ . The method to normalize the SPT  $N$ -value with effective overburden stress (Eq. (2)) and the method to adjust the  $N_1$  value by taking into account the effect of the fines content (Eq. (7)) should be studied further.

- 4) The shear modulus,  $G$ , obtained in the laboratory tests increased approximately 40% due to sand compaction. The effects of sand compaction on the damping ratio ( $h$ ) were negligible. The effects of sand compaction on the strain dependence of shear modulus ( $G/G_0 \sim \gamma$ ) and damping ratio ( $h \sim \gamma$ ) were essentially negligible. Unlike the increase in  $G_0$  due to sand compaction measured in laboratory tests, no significant increase in shear wave velocity was observed for sand at depths of from 1 to 5 m, even after sand compaction. The disharmony in the effect of sand compaction on  $G$  between the laboratory test results and the field test results at this depth cannot be explained at present and should be studied further.

## ACKNOWLEDGEMENTS

The present study was supported financially by the Ministry of Education, Culture, Sport and Science of Japan. The authors would also like to thank Messrs, S. Oh-daka, D. Kikuta, and A. Fujita, graduate students of the Chiba Institute of Technology, for their assistance in performing the laboratory tests.

## REFERENCES

- 1) Architectural Institute of Japan (2001): *Recommendations for Design of Building Foundations*, 62–63 (in Japanese).
- 2) Harada, K., Yamamoto, M. and Ohbayashi, J. (1997): A consideration on the increase of  $K_0$ -value in the sand improved by static sand compaction pile method, *Proc. 52nd Annual Meeting of Japanese Society of Civil Engineers*, 540–541 (in Japanese).
- 3) Harada, K., Yamamoto, M. and Yasuda, S. (2000): Influence of earth pressure coefficient on SPT  $N$ -value and liquefaction resistance of the ground improved by compaction method, *Annual Meeting of AIJ*, 669–670 (in Japanese).
- 4) Hatanaka, M. and Feng, L. (2006): Estimating relative density of sandy soils, *Soils and Foundations*, 46(3), 299–313.
- 5) Hatanaka, M. and Uchida, A. (1996): Empirical correlation between penetration resistance and internal friction angle of sandy soils, *Soils and Foundations*, 36(4), 1–9.
- 6) Hatanaka, M., Uchida, A. and Oh-oka, H. (1995): Correlation between the liquefaction strengths of saturated sand obtained by in-situ freezing method and rotary-type triple tube method, *Soils and Foundations*, 35(2), 67–75.
- 7) Hatanaka, M., Uchida, A., Kakurai, M. and Aoki, M. (1998): A consideration on the relationship between SPT  $N$ -value and internal friction angle of sandy soils, *J. Struct. Constr. Eng.*, AIJ, (506), 125–129 (in Japanese).
- 8) Ishihara, K. (1977): State-of-the-Art Report on the Stress-Deformation and Strength Characteristics, *Proc. 9th ICSMFE*, 2, 424–426.
- 9) Ishihara, K. and Yasuda, S. (1975): Sand liquefaction in hollow cylinder torsion under irregular excitation, *Soils and Foundations*, 15(1), 45–59.
- 10) Ishihara, K., Iwamoto, A., Yasuda, S. and Takasu, H. (1979): Liquefaction of anisotropically consolidated sand, *Proc. 9th ICSMFE*, 11–15.
- 11) Japan Highway Association (2002): *Instruction and Explanation for Inspection of Highway Bridge Design*, Parts 1 and 4, 564–566 (in Japanese).
- 12) Ohbayashi, J., Harada, K. and Yamamoto, M. (1999): Resistance against liquefaction of ground improved by sand compaction pile method, *Proc. 2nd International Conference on Earthquake and Geotechnical Engineering*, 2, 27–33.
- 13) Okamura, M., Ishihara, M. and Ohshita, T. (2004): Liquefaction resistance of sand deposit improved with sand compaction piles, *Soils and Foundations*, 43(5), 175–187.
- 14) Tokimatsu, K. and Yoshimi, Y. (1983): Empirical correlation of soil liquefaction based on SPT  $N$ -value and fines content, *Soils and Foundations*, 23(4), 56–74.
- 15) Tokimatsu, K., Yoshimi, Y. and Ariizumi, K. (1990): Evaluation of liquefaction resistance of sand improved by deep vibratory compaction, *Soils and Foundations*, 30(3), 153–158.
- 16) Yamamoto, M., Harada, K. and Nozu, M. (2000): A new method for designing sand compaction pile method for loose sandy soils, *Tsuchi-to-Kiso*, 48(11), 17–20 (in Japanese).
- 17) Yoshimi, Y. (1994): Relationship among liquefaction resistance, SPT  $N$ -value and relative density for undisturbed samples of sands, *Tsuchi-to-Kiso*, 42(4), 63–67 (in Japanese).
- 18) Yoshimi, Y., Hatanaka, M. and Oh-oka, H. (1978): Undisturbed sampling of saturated sand, *Soils and Foundations*, 18(3), 59–73.